Supporting Information

Hierarchical TiO_2 Nanostructured Array/P3HT Hybrid Solar Cells with Interfacial Modification

Wen-Pin Liao, Shu-Chien Hsu, Wan-Hsien Lin and Jih-Jen Wu*

Department of Chemical Engineering, National Cheng Kung University, Tainan 701, Taiwan

Characterizations of TiO_2 NR arrays on FTO substrates

X-ray diffraction (XRD) patterns of the NR arrays are shown in Figure S1(a). In addition to the diffraction peaks corresponding to the FTO substrate, the diffraction peaks of the NR array are pertaining to those of rutile TiO_2 phase according to the ICDD-PDF No. 01-088-1175. Moreover, Figure S1(b) reveals that the peaks at 265, 429 and 606 cm^{-1} observed in the Raman spectra of the TiO_2 NR array are pertaining to Raman shift peaks of the rutile TiO_2 structure. Both XRD and Raman characterizations demonstrate the formation of rutile TiO_2 NR array on the FTO substrate. Further structural characterizations of the TiO_2 NRs are performed using transmission electron microscopy (TEM). The high-resolution (HR) TEM image and the corresponding selected area electron diffraction (SAED) pattern of an individual NR are shown in Figure S1(d) and S1(e). They illustrate that the NR possesses a single-crystalline structure of rutile TiO_2. Figure S1(d) shows that the lattice spacing of ~ 2.94 nm along the longitudinal axis direction pertains to the d-spacing of rutile TiO_2 (001) crystal planes. Additionally, Figure S1(d) reveals that NPs formed on the surface of NR by $TiCl_4$ treatment possess rutile TiO_2 structure as well.

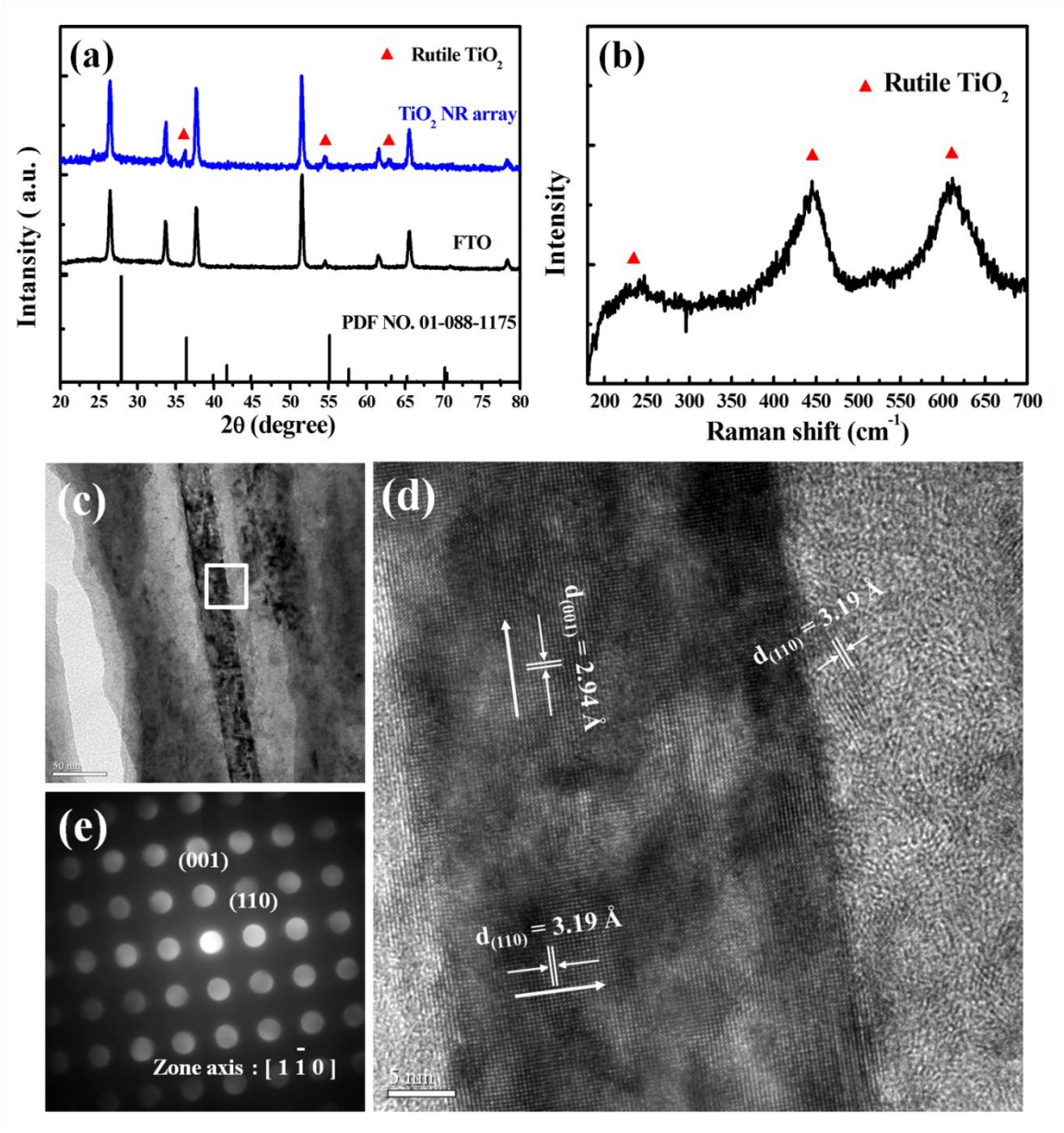

Figure S1. (a) XRD patterns and (b) Raman spectra of TiO_2 array on FTO substrate. (c) TEM image of TiO_2 NRs. (d) High-resolution cross-sectional TEM image and (e) the corresponding selected area electron diffraction pattern of TiO_2 NR.

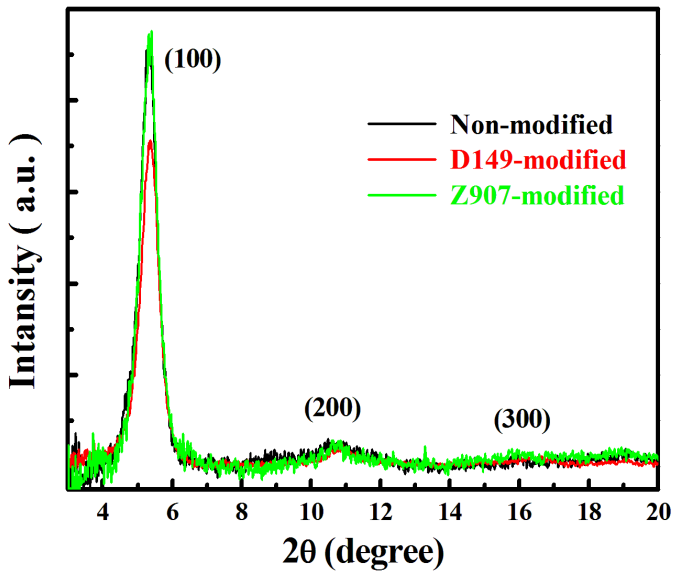

Figure S2. (a) XRD patterns of P3HT infiltrated in dye-modified and non-modified TiO_2 NR arrays.

Determination of the band diagrams of the P3HT/dye/TiO_2 NR hybrids

The non-equilibrium band diagrams of the hybrids are determined using the following procedure. First of all, the energy band gaps (E_g) of the dye molecules and P3HT are determined using absorption spectra shown in Figure 2(b). The band gaps of Z907, D149 and P3HT are estimated to be 2.05, 1.97 and 1.91 eV, respectively. The HOMO energy levels of the dye molecules are then determined by cyclic voltammetry (CV) measurements. The CV measurements were performed in acetonitrile solution containing the supporting electrolyte of tetrabutylammonium hexafluorophosphate ($TBAPF_6$, 0.1 M). The dye-adsorbed or P3HT infiltrated TiO_2 NR array, a platinum wire and a nonaqueous $Ag/AgNO_3$ electrode (0.56 V vs. NHE) were used as the working, counter and reference electrodes, respectively. Figure 3(a) shows the CV results of D149 adsorbed on TiO_2 NRs and P3HT infiltrated in TiO_2 NR array. The HOMO energy levels (E_{HOMO}) and lowest unoccupied molecular orbital (LUMO) energy levels (E_{LUMO}) of the dye molecules adsorbed on TiO_2 NRs and P3HT infiltrated in TiO_2 NR array were estimated using the relations of

$$E_{HOMO} = (-5.06 - E_{onset} + \Delta E_n)eV \quad (1)$$

$$E_{LUMO} = (E_{HOMO} + E_g)eV \quad (2)$$

where -5.06 eV is the redox potential of $Ag/AgNO_3$ vs. vacuum level, E_{onset} is the oxidation onset potential obtained from CV measurement and ΔE_n is the energy difference between conduction band edge (E_{C,TiO_2}) and Fermi level (E_{F,TiO_2}) of TiO_2 NR. E_{C,TiO_2} is -4.2 eV by referring literature report.[1] E_{F,TiO_2} is measured to be 4.61 eV using Kelvin probe force microscope (KPM). E_{HOMO} and E_{LUMO} of D149 and Z907 adsorbed TiO_2 NR arrays and P3HT

infiltrated in TiO_2 NR array are listed in Table S1. Figure 3(b) shows the non-equilibrium band diagram of the TiO_2 NR array/D149/P3HT hybrid using the data in Table S1.

Table S1. Non-equilibrium energy level positions determined by CV and KPM measurements

TiO_2 NR	E_{onset} (V *vs.* $Ag/AgNO_3$)	E_{HOMO} (CV) (eV)	E_{LUMO} (CV) (eV)	$E_{w,KPM}$ (eV)
Bare	- -	- -	- -	4.61
D149-absorbed	0.46	-5.11	-3.14	4.10
Z907-absorbed	0.83	-5.48	-3.43	4.23
P3HT-infiltrated	0.43	-5.08	-3.17	4.35

To estimate the HOMO energy levels of the dyes in the hybrids at equilibrium, the TiO_2 NR array/dye/P3HT hybrids, instead of the dye-adsorbed TiO_2 NR arrays, were employed to be working electrodes for the CV measurements. The result of TiO_2 NR array/D149/P3HT hybrid is shown in Figure 3(c). Since the E_{HOMO} of P3HT is higher than that of dye molecules, the E_{onset} obtained from the CV result is attributed to the oxidation of the dye molecule. Consequently, the HOMO energy levels of the dyes in the TiO_2 NR array/dye/P3HT hybrids at equilibrium can be determined by eq. (1) using the E_{onset} shown in Figure 3(c). The LUMO energy levels of the dyes are then obtained using eq. (2).

On the other hand, the HOMO energy levels of P3HT in the hybrids at equilibrium are estimated by the relation of

$$E_{HOMO,P3HT} = -(E_{W,hybrid} + \Delta E_p)eV \qquad (3)$$

where $E_{W,hybrid}$ is the work function of the TiO_2 NR array/dye/P3HT hybrid and ΔE_p is the energy difference between the valance band edge $(E_{v,P3HT})$ and Fermi level $(E_{F,P3HT})$ of P3HT. Here, ΔE_p taken from literature is 0.28 eV,[2] in which employed P3HT was purchased from the same company and was dissolved in the same solvent as done in this work. $E_{W,hybrid}$ of the TiO_2 NR array/dye/P3HT hybrids are determined by KPM. Because the variation exists between the same energy level measured by KPM and CV, the offset should be calibrated in order to integrate the data obtained from both measurements. In this work, the calibration is based on the Fermi level of P3HT infiltrated in TiO_2 NR array. The work function of the P3HT/TiO_2 NR array measured by KPM is 4.35 eV. On the other hand, the HOMO energy level of P3HT infiltrated in the TiO_2 NR array determined by CV is -5.08 eV. By adding up the ΔE_p, The work function of the P3HT/TiO_2 NR array attained from CV measurement is 4.8 eV. As a result, the KPM-measured energy level should be calibrated by an offset of 0.45 eV. The calibrated $E_{W,hybrid}$ of the TiO_2 NR array/dye/P3HT hybrids are shown in the $E_{W,calibrated}$ column of Table S2. Therefore, the HOMO and LUMO energy levels of P3HT in the TiO_2 NR array/dye/P3HT hybrids at equilibrium are calculated by eq. (3) and (2), respectively.

REFERENCE

(1) Yoshitake, H.; Abe, D. *Microporous Mesoporous Mat.,* **2009**, *119*, 267.

(2) Davis, R. J.; Lloyd, M. T.; Ferreira, S. R.; Bruzek, M. J.; Watkins, S. E.; Lindell, L.; Sehati, P.; Fahlman, M.; Anthony, J. E.; Hsu, J. W. P. *J. Mater. Chem.*, **2011**, *21*, 1721.

Table S2. Equilibrium energy band levels determined by CV and KPM measurements

TiO_2 NR/P3HT hybrid	E_{onset} (V *vs.* $Ag/AgNO_3$)	$E_{HOMO,\ dye}$ (eV)	$E_{LUMO,\ dye}$ (eV)	$E_{W,KPM}$ (eV)	$E_{W,calibrated}$ (eV)	$E_{HOMO,\ P3HT}$ (eV)	$E_{LUMO,\ P3HT}$ (eV)
Non-modified	0.43	- -	- -	4.35	4.80	-5.08	-3.17
D149-modified	0.74	-5.39	-3.42	3.82	4.27	-4.55	-2.64
Z907-modified	0.91	-5.56	-3.51	3.98	4.43	-4.71	-2.80

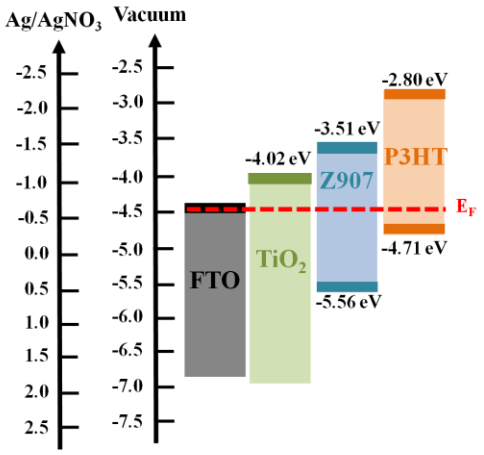

Figure S3. Equilibrium energy band diagram of TiO_2 NR array/Z907/P3HT.

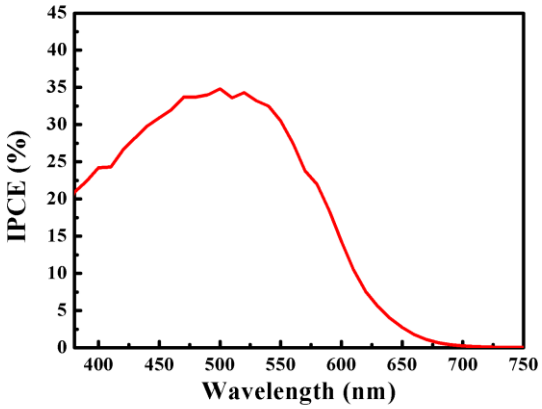

Figure S4. IPCE spectrum of D149-modified TiO_2 NR array/P3HT solar cell.

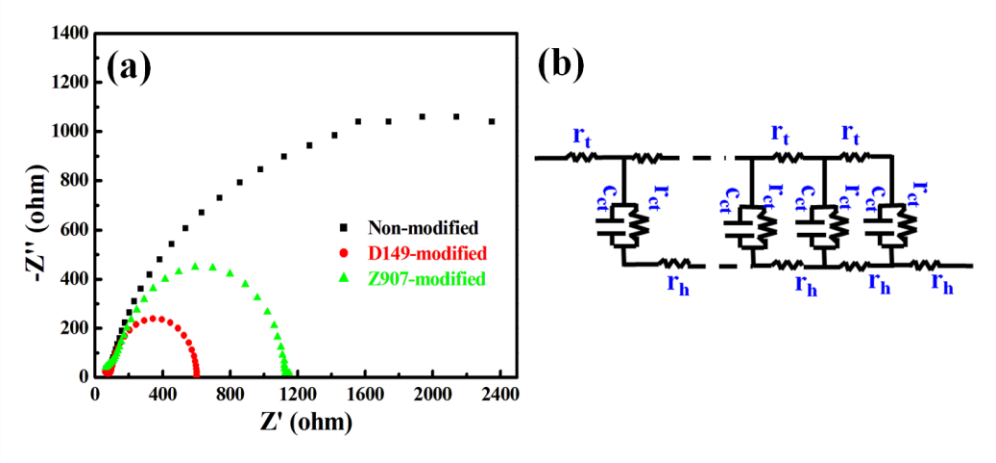

Figure S5. (a) Nyquist plots of non-modified, D149-modified and Z907-modified TiO_2 NR array-P3HT cells. (b) Suggested equivalent circuit of the heterojunction hybrid solar cells. R_t (= $r_t \times$ L) is the electron transport resistance in TiO_2 NRs (L is the length of TiO_2 NRs), R_{ct} (= r_{ct} / L) is the charge transfer resistance related to recombination at the TiO_2/P3HT interface, C_μ (= $c_\mu \times$ L) is the chemical capacitance related to double layer at the interface, R_h (= $r_h \times$ L) is the hole transport resistance in P3HT film, respectively.

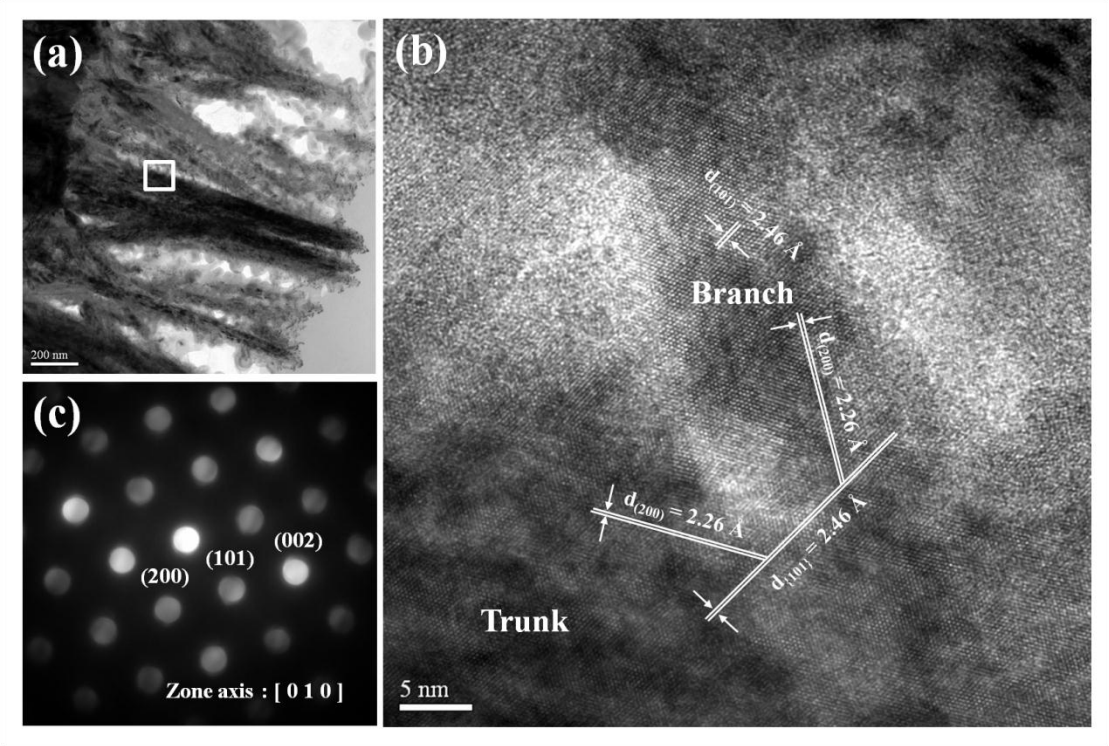

Figure S6. (a) TEM image of TiO_2 ND array. (b) High-resolution cross-sectional TEM image of ND and (c) the corresponding selected area electron diffraction pattern of the trunk region in (b).